Stepwise treatment of ashes and slags by dissolution, precipitation of iron phases and carbonate precipitation for production of raw materials for industrial applications

Daniel Höllen, Iris Berneder, Francesca Capo Tous, Markus Stöllner, Klaus Philipp Sedlazeck, Therese Schwarz, Alexia Aldrian, Markus Lehner

Angaben zur Veröffentlichung / Publication details:

Höllen, Daniel, Iris Berneder, Francesca Capo Tous, Markus Stöllner, Klaus Philipp Sedlazeck, Therese Schwarz, Alexia Aldrian, and Markus Lehner. 2018. "Stepwise treatment of ashes and slags by dissolution, precipitation of iron phases and carbonate precipitation for production of raw materials for industrial applications." *Waste Management* 78: 750–62. https://doi.org/10.1016/j.wasman.2018.06.048.

Stepwise treatment of ashes and slags by dissolution, precipitation of iron phases and carbonate precipitation for production of raw materials for industrial applications

Daniel Höllen [a,*], Iris Berneder [b], Francesca Capo Tous [b], Markus Stöllner [a], Klaus Philipp Sedlazeck [a], Therese Schwarz [a], Alexia Aldrian [a], Markus Lehner [b]

[a] Chair of Waste Processing Technology and Waste Management, Montanuniversität Leoben, Franz-Josef-Str. 18, 8700 Leoben, Austria
[b] Chair of Process Technology and Industrial Environmental Protection, Montanuniversität Leoben, Franz-Josef-Str. 18, 8700 Leoben, Austria

1. Introduction

1.1. Recycling of ashes and slags

1.1.1. Recycling of ashes

Ashes represent a huge mineral waste stream, especially in industrialised countries, which is still mostly landfilled due to heavy metal and chloride contents (Austrian Federal Ministry of Agriculture, 2017). The chemical and mineralogical composition of combustion residues as well as the content and availability of heavy metals depend on the feed material and thermal treatment applied (Koukouzas et al., 2006; Ljung and Nordin, 1997; Vassilev et al., 2013a,b; Piantone et al., 2004).

The increase in the energetic use of biomass led to increasing production of biomass ashes from 100.000 t/a in 2004 to 186.000 t/a in 2015 (Austrian Federal Ministry of Agriculture, 2017). Collection logistics are rather difficult as biomass ashes (BA) are produced at more than 1100 different sites in Austria, among which only 10 have a thermal power production of more than 10 MW (Pleßl, 2015). 50% of BA are landfilled in Austria (BMLFUW, 2014a,b), because heavy metals and chloride contents limit their application as soil amendment (Vassilev et al., 2013a,b) and material for cement production (Obernberger and Supancic, 2009).

In 2012, 882.400 t of municipal solid waste incineration (MSWI) ashes were produced in Austria, thereof 579.00 t bottom or bed

* Corresponding author.
E-mail address: daniel.hoellen@unileoben.ac.at (D. Höllen).

ashes and 303.400 t fly ashes (BMLFUW, 2014a,b). Theoretically, the recycling of MSWI bottom ashes (MSWI-BA) in road construction is possible in Austria (Austrian Federal Ministry of Agriculture, 2017). Due to specific conditions, i.e. the abundance of natural rocks and lack of acceptance of MSWI-BA utilisation (Environmental Agency Austria, 2005) 100% of MSWI ashes are disposed of at landfills in Austria (Bundesministerium für Land- und Forstwirtschaft, Umwelt und Wasserwirtschaft, 2015). Limitations for the recycling of MSWI-BA are mainly due to its content and leaching of soluble components like salts and/or some heavy metals, which might have a negative effect on the environment and/or industrial installations like cement kilns. To avoid these negative effects, washing processes have been successfully conducted to remove chlorides (Pan et al., 2008) and heavy metals like Cd and Zn (Mulder, 1996) from MSWI-BA. However, as leaching depends on the solubility of mineral phases, the mineralogy of ashes must be changed to decrease leaching, e.g. by the incorporation of heavy metals in stable mineral phases (Nzihou and Sharrock, 2002).

Paper sludge incineration ashes (PSI-A) result from the combustion of fibre residues from waste paper recycling. Their annual production is significantly smaller than that of MSWI-BA and there are already existing recycling opportunities like amendment for soil improvement (Muse and Mitchell, 1995).

1.1.2. Recycling of slags

In Austria, 94.000 t electric arc furnace slags (EAF-S) are produced yearly. Mineralogically, stainless steel slags from EAF processes are composed of Ca-, Al- and Mg-silicates, Ca-, Mg- and Fe-oxides, Ca-ferrites, spinels, aluminates and fluorides (Drissen, 2004). Road construction is the main application of EAF-S (Engström et al., 2014), but the Austrian legislation (Republik Österreich, 2015) sets strict limit values for both total and leachable contents of environmentally relevant elements. Consequently, even advanced methods to reduce the leachability of steel slags (Cabrera-Real et al., 2012) will not allow increased slag recycling under present legal framework conditions. To solve this problem a pyrometallurgical reduction of the slag followed by magnetic separation of the produced zero-valent metals has been suggested (Adamcyzk et al., 2010).

Aside from slags, which account for 75% of all metallurgical residues, dusts and sludges represent a smaller group of materials (7%, (Gara and Schrimpf, 1998)). Steel dusts, which are also considered in this study, can partly be internally recycled (Chairaksa-Fujimoto et al., 2015), but in 2015, 25% were still landfilled in Austria (Austrian Federal Ministry of Agriculture, 2017).

1.2. Mineral carbonation

Mineral carbonation is the exothermic reaction of carbon dioxide with metal oxides or silicates to form carbonates according to the general formula:

$$Me^{2+}O(s) + CO_2(g) \rightarrow MeCO_3(s) \Delta H_R^0 < 0 \quad (1)$$

The theoretical CO_2 uptake, T_{CO2}, is defined as the maximum amount of CO_2 that can be bound in a material, expressed as percentage referred to the mass of the input material (Sanna et al., 2012):

$$T_{CO2} = 0.79 \times (\%CaO - 0.56 \times CaCO_3) + 1.09 \times \%MgO \quad (2)$$

Carbonation of alkaline residues is well known and an important factor in the long-term behaviour of ashes (Meima et al., 2002) and slags (Suer et al., 2009). However, in natural environments, ashes and slags carbonate only at the surface even after 10 years of ageing in a road (Suer et al., 2009). This is due to the lower reactivity of silicates and complex oxides compared to free lime (Costa et al., 2007; Sanna et al., 2014) and due to the clogging effect of the formed carbonates. The following equation summarizes the carbonation reaction of larnite, a calcium silicate:

$$Ca_2SiO_4 + 2CO_2 \rightarrow 2CaCO_3 + SiO_2 \quad (3)$$

In order to effectively employ carbonation for carbon capture, utilisation and storage (CCUS) an indirect process route may be applied. This process is made up by a first stepaimed at the dissolution of the primary silicate mineral phase (4) followed by the precipitation of the carbonate mineral phases (5).

$$Ca_2SiO_4(s) + H_2O(l) + 4H^+ \rightarrow H_4SiO_4(aq) + H_2O(l) + 2Ca^{2+}(aq) \quad (4)$$

$$Ca^{2+}(aq) + CO_2(aq) \rightarrow CaCO_3(s) \quad (5)$$

This decoupling of the reactions allows for inserting an additional reaction in the aqueous solution to precipitate metals which would decrease the purity of the desired carbonate product:

$$Fe^{3+}(aq) + 3OH^- \rightarrow Fe(OH)_3(s) \quad (6)$$

1.3. Objectives of the work

Carbon dioxide is the fifth most abundant gas in the atmosphere and its emission is the main cause for global warming, whereas slags and ashes are significant waste streams in Europe. In this study we present an approach for achieving a substantial conversion of ashes and slags into carbonates via dissolution and precipitation, which aims to trap CO_2 and to recover metals in different insoluble mineral phases via a multi-step reaction route.

The aim of this work is to apply this stepwise treatment to different types of poorly valorised industrial residues to assess which may be the most promising ones to employ for the process, in terms of total content of specific elements in the obtained products. All the newly produced side and end products from this process should be utilised in various industrial applications. The proposed stepwise treatment aims to achieve the following objectives:

1. Recycling of those ashes and slags which are currently disposed of in landfills due to their high total and/or leachable heavy metal concentrations and/or due to their poor mechanical properties.
2. Reduction of the CO_2 emissions of Waste-to-Energy plants and other energy-intensive industrial plants by carbon capture, utilisation and storage (CCUS).
3. Production of precipitated calcium carbonate (PCC) as a substitute for primary resources as building material and filler (e.g. in paper industry).
4. Production of a SiO_2 concentrate to be used as an aggregate for building materials.
5. Hydrometallurgical recovery of ferrous metals for the steel industry.

This approach is based on an indirect process where dissolution and precipitation reactions are decoupled (Eloneva et al., 2012) in order to enable faster reaction kinetics, as the release of Ca into the solution is the rate-limiting reaction step (Huijgen et al., 2005) and without decoupling the surface would be passivated by the reaction products.

2. Material and methods

2.1. Material characterisation

In this study we present a complete experimental procedure to produce precipitated calcium carbonate from slags and ashes which included mechanical processing for removal of metallic pieces and increasing the specific surface area for subsequent reactions, incongruent dissolution for selective extraction of Ca leaving behind a siliceous residue, precipitation of iron compounds for metallurgical recycling and precipitation of carbonates as industrial raw materials from the remaining solution (Fig. 1).

Samples were selected based on chemical, physical and mineralogical properties and waste management aspects. Chemical properties included high calcium and low heavy metal contents, while physical properties regarded a fine grain size or a good crushability to less than 100 μm and a low content of ductile materials. Mineralogical properties were a high and selective solubility of Ca-containing phases and waste management aspects comprised a high availability at low costs and a lack of existing recycling opportunities. Two residues from stainless steel production and three residues from incineration processes were selected:

1. EAF slag from stainless steel production (EAF-S)
2. EAF filter dust from stainless steel production (EAF-FD)
3. Biomass combustion bottom ash (BC-BA)
4. Treated MSWI bottom ash (MSWI-BA)
5. Paper sludge incineration ash (PSI-A)

The processed MSWI-BA sample was taken at a waste treatment plant in Austria by shovels at different locations in an ash heap, digging as deep as possible into the heap. However, the representativeness of the sample for the heap was limited because the interior could not be sampled. All other samples were obtained directly from industrial partners. Sample amounts accounted for 6–15 kg, depending on the grain size of the material. The representativeness of the samples for a certain batch or a yearly production could not be validated, so the results were only valid for the sample itself and not for whole waste streams.

Thin sections for microscopic investigations were prepared from unprocessed samples. Mechanical processing of the EAF-S, MSWI-BA and BC-BA was conducted with a hammer (for EAF-S only), a jaw crusher (Fritsch Pulverisette 1, Type 01703, d = 8 mm) and a hand magnet (if necessary). No comminution was required for PSI-A and EAF-FD. Quartering of the sample by a ripple divider yielded representative subsamples for grinding with a planet ball mill (Fritsch Pulverisette 5, Type 05.202, t = 12 min). After sieving (d = 125 μm and d = 1000 μm), grinding was repeated for the middle fraction to increase the yield of the fraction <125 μm to 78–89 wt% of the original sample. The fraction <63 μm was separated by sieving and the fraction 63–125 μm was used for the experiments. This very specific grain size fraction was used in the tests because the methodology was the same as that adopted for dissolution tests carried out on serpentine samples. Consequently, the same particle size fraction was tested for all residues to evaluate the results achievable as a function of the chemical composition and mineralogy of the different residues and not of physical characteristics. Subsamples of this fraction were taken by a riffle divider and were further ground to <63 μm for chemical and mineralogical analyses using an agate mortar mill (Fritsch Pulverisette 2, Nr. 02.105/5147). Chemical and mineralogical analyses were performed for both metallurgical slags and ashes from waste and biomass incineration. The bulk chemistry of main components was investigated by X-ray fluorescence analyses (XRF, AXIOS, DIN

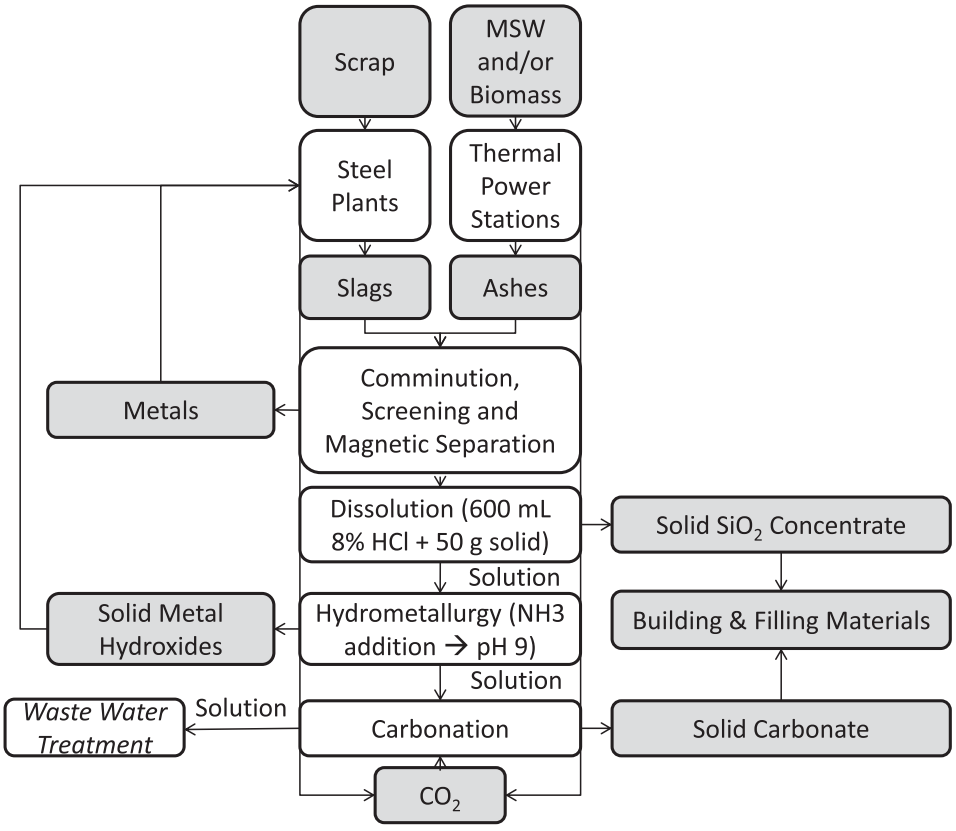

Fig. 1. Objective of the work.

EN ISO 12677) using lithium tetraborate melt tablets. The initial organic and inorganic carbon content was determined according to ÖNORM EN 13137 where the total carbon (TC) was incinerated and determined via infrared spectroscopy, the total inorganic carbon (TIC) was determined by acidification and quantification of the evolved CO_2 by infrared measurement, whereas the total organic carbon (TOC) was calculated as the difference. Trace elements were determined by inductively coupled plasma mass spectroscopy (ICP-MS, Agilent 7500 cx, after a microwave-assisted total digestion using a mixture of HF, HNO_3 and HCl according to ÖNORM EN 13656). The bulk mineralogy was investigated by X-ray powder diffraction (Bruker D8 Advance, Cu Kα, Software Diffrac.eva v3.2). Obtained results were confirmed by Raman spectroscopy (Jobin Yvon (Horiba) LabRAM, Nd-YAG laser, 532 nm) and reflected and transmitted light microscopy (Zeiss Axio Scope A1). The crystal chemistry of relevant phases for mineral carbonation was analysed by electron microprobe analyses (Jeol JXA 8200 Superprobe).

2.2. Dissolution experiments

50 g of the well characterized materials were dissolved in 600 mL hydrochloric acid (8%) for 180 min at 90 °C. The solid:liquid ratio (8–50 g solid per 600 mL) and the kind (HCl vs H_2SO_4) and concentration (4–19%) of acid were varied in preliminary experiments and the chosen parameters were the optimum balance between minimum consumption of chemicals and maximum extraction efficiency. Gravity filtration and centrifuge technologies were used for separation of solids and aqueous solutions. Filters were rinsed with double distilled water and the washing water and the filtrate were analysed separately for their chemical composition using inductively coupled plasma mass spectroscopy (ICP-MS, Agilent 7500 cx).

Acid recovery by diffusion dialyses (Fumatech FT-DD-200-5) was tested for a selected acidic solution obtained from an experiment using serpentinite (V = 3 L, pH = −0.3, electric conductivity = 341 μS/cm), which is a membrane procedure where the acidic solution is subjected to a counterflow of deionised water (t = 8 h, Q = 446 mL/h), and compared with a reference experiment with neutralisation by NH_3 addition only.

Dissolution residues were dried for 24 h at 105 °C and removed from the filter. Sections for electron microprobe analyses were produced by embedding the residues in epoxy resin. Another fraction was ground to destroy aggregates formed during drying using an agate mortar. The dissolution residues were analysed by XRD, EMPA (residues of EAF-S, MSWI-BA, BC-BA) and after total digestion according to ÖNORM EN 13656 also by ICP-MS in the same way as the input materials.

A mass balance of dissolution experiments was conducted by multiplying the concentrations of individual elements in the product fractions, i.e. acidic solution and dissolution residue, with the masses of the individual fractions. Finally the resulting sums were compared with the amounts of individual elements which should have been present according to chemical analyses of input materials.

2.3. Precipitation experiments

Aqueous solutions resulting from dissolution experiments were strongly acidic. To remove the acid, dissolved ammonia (NH_3) was added, until a pH of 9 was reached. Titration was stopped and resulting precipitates were removed from the solution by filtration (0.45 μm).

The precipitates were investigated mineralogically by XRD and EMPA (EAF-S, BC-BA, MSWI-BA, PSI-A), whereas for chemical analyses total digestion was conducted and the resulting solutions were analysed by ICP-MS in the same way as the input material. The mass balance was calculated like described for dissolution experiments.

2.4. Carbonation experiments

After the precipitation experiments, CO_2 was introduced into the remaining solution with a flow rate of 0.11 L/s. The pH was kept constant (at pH of 9) by simultaneous addition of NH_3. The influx of CO_2 and NH_3 was stopped when carbonation was complete. The completion was concluded from the titration curve, i.e., more NH_3 had to be added to keep the pH constant because CO_2 was not consumed for carbonate precipitation, but remained in the solution causing acidification of the solution. The precipitates were separated from the solution by filtration (0.45 μm), washed with ultrapure water, dried for 24 h at 40 °C and analysed for total inorganic carbon according to ÖNORM 13137. The samples were digested totally and the chemical composition was determined by ICP-MS. The solid phases were identified by XRD and EMPA (carbonates produced from EAF-S, MSWI-BA, BC-BA, PSI-A) as described for the input materials. The $CaCO_3$ content was investigated according to DIN EN ISO 3262-1. The mass balance was calculated like described for the dissolution experiments.

3. Results and discussion

3.1. Material characterisation

The chemical composition of the selected materials varied significantly (Table 1). CaO contents were in the range of 13–54 wt%. Major components were Fe_2O_3 (+ Fe + FeO, which were calculated together as Fe_2O_3) for residues from the steel industry and SiO_2 for residues from incineration. MgO was only a minor component and consequently might only play a minor role for the CO_2 binding capacity. The chemical composition of the investigated EAF–S was in the range of a broad comparative study on these materials (Rekersdrees et al., 2014), but more alkaline compared to another German study (Drissen, 2004). The investigated MSWI-A was similar to literature values from Austria (Lechner and Huber-Humer, 2011), but had lower CaO contents than reported for a Taiwanese material (Pan et al., 2008). Regarding BC-BA, the determined chemical composition lied between that of bark and straw ashes (Obernberger et al., 1997) which suggests the use of mixed fuels in the respective plant.

Mineralogical investigations showed that Ca, which was the target element for carbonation, was mainly bound in calcium ferrites and aluminates in residues from the steel industry and in calcium silicates in ashes (Table 2).

Typically, EAF-S consisted of a heterogeneous mixture of dark and light materials. The dark material obtained its colour from the high FeO content and was similar to that described as "black EAF slag" (Rekersdrees et al., 2014) and as "EAF slag C" (Shi, 2004). The light material was composed of free lime and possibly also secondary metallurgical slags. As only the dark material was assumed to truly originate from the EAF process, only this material was used for mineral carbonation experiments. The CaO content of this dark material (EAF-S) accounts for 31 wt% which corresponded - including the low MgO content of 5.4 wt% - to a CO_2 binding capacity of 30% using Eq. (2). Ca was present in the slag predominantly as brownmillerite, alite, melilite and mayenite but also as belite/larnite, cuspidine, ettringite, scheelite, fluorite, portlandite, and calcium chromite (Table 2). However, the main phase in the slag was Mn-containing magnesiowustite, which was almost the only Mg-phase. Additionally, spinels, olivine, corundum and metallic iron were identified.

Table 1
Chemical composition of slags and ashes (wt%, *italics: ICP-MS*, * *AAS (external data)*, # *(external data, various methods)*, concentrations < 0.01 wt% are displayed as such independent from the actual limit of detection which was smaller in any case,; n.a.: not analysed).

Parameter	EAF-S	EAF-FD	MSWI-BA	BC-BA	PSI-A#
CaO	30.67	36.41	20.97	27.17	54.25
MgO	5.39	8.57	3.70	5.32	3.50
SiO_2	9.35	6.25	41.30	48.19	20.90
Al_2O_3	5.77	0.81	10.87	5.75	10.86
Fe_2O_3	37.13	27.66	14.03	3.22	1.05
Cr_2O_3	6.62	11.91	0.20	0.03	*<0.01*
MnO	4.03	5.14	0.27	0.53	0.04
TiO_2	0.15	0.12	1.07	0.40	n.a.
P_2O_5	0.22	0.11	0.75	1.80	0.61
K_2O	0.03	0.37	0.81	6.41	0.51
Na_2O	0.16	0.41	2.84	0.79	0.44
ZnO	0.03*	0.88	0.23	*0.01*	*0.06*
CuO	0.01*	0.24	0.30	*0.02*	*0.05*
PbO	*<0.01*	*0.03*	*0.03*	*<0.01*	*0.02*
V_2O_5	*0.30*	*1.00*	*<0.01*	*0.03*	*<0.01*
MoO_3	*0.17*	*4.47*	*0.01*	*<0.01*	*<0.01*
WO_3	*0.11*	*0.30*	*<0.01*	*0.01*	n.a.
SO_3	0.24	<0.04	1.10	0.06	1.00
L.O.I.	n.a.	7.80	2.09	0.06	9.27
CO_2	<1.83	9.90	2.57	<3.67	n.a.

Table 2
Mineralogical composition of slags and ashes (Identification by a combination of reflected and transmitted light microscopy, electron microprobe analyses, Raman spectroscopy and X-ray diffraction, estimation of quantities (−: absent; +: minor amounts; ++: intermediate amounts; +++: major amounts)).

Phase/formula	EAF-S	EAF-FD	MSWI-BA	BC-BA	PSI-A
Metallic iron, Fe	+	–	+	+	–
Metallic aluminium, Al	–	–	+	–	–
Amorphous silica, SiO_2	–	–	+	–	–
Metallic copper, Cu	–	–	+	–	–
Bronze, CuZn	–	–	+	–	–
Ferrosilicon, FeSi	–	–	+	–	–
Idaite, Cu_3FeS_4	–	–	+	–	–
Fluorite, CaF_2	+	+	–	–	–
Mn-containing Magnesiowustite, (Mg,Fe,Mn)O	+++	+	+	–	–
Lime, CaO	–	–	–	–	+
Hematite, α-Fe_2O_3	–	+++	+	–	–
Brownmillerite, $Ca_2(Al,Fe,Cr)_2O_5$	++	–	+	–	–
Corundum, α-Al_2O_3	+	–	+	–	–
Zircon, $ZrSiO_4$	–	–	–	+	–
Spinel, $(Fe,Mg,Mn)(Al,Cr)_2O_4$	+	+++	–	–	–
Magnetite, Fe_3O_4	–	–	+	–	–
Mayenite, $Ca_{12}Al_{14}O_{33}$	++	–	–	+	–
Tricalciumaluminate, $Ca_3Al_2O_6$	+	–	–	–	++
Calciochromite, $CaCr_2O_4$	+	–	–	–	–
Portlandite, $Ca(OH)_2$	+	++	+	+	+
Gibbsite, γ-$Al(OH)_3$	–	–	+	–	–
Calcite, $CaCO_3$	–	++	+++	++	++
Dolomite, $CaMg(CO_3)_2$	–	–	+	++	–
Anhydrite, $CaSO_4$	–	–	+	–	–
Ettringite, $Ca_6Al_2[(OH)_{12}](SO_4)_3{\cdot}26H_2O$	+	–	+	–	–
Powellite, $CaMoO_4$	–	++	–	–	–
Scheelite, $CaWO_4$	+	–	–	–	–
Apatite, $Ca_5[(F,Cl,OH)(PO_4)_3]$	–	–	–	+	–
Larnite, β-Ca_2SiO_4	+	–	+	+	–
Calcio-Olivine, γ-Ca_2SiO_4	–	–	–	–	+++
Olivine, $(Fe,Mg)_2SiO_4$	+	–	+	–	–
Alite/C_3S, Ca_3SiO_5	++	–	–	–	–
Melilite, $(Ca,Na)_2(Al,Mg,Fe)(SiAl)_2O_7$	++	–	+++	+++	++
Cuspidine, $Ca_4Si_2O_7(F,OH)_2$	+	–	–	–	–
Wollastonite, $CaSiO_3$	–	–	+	+	–
Ferrosilite, $Fe_2Si_2O_6$	–	+	–	–	–
Biotite, $K(Mg,Fe)_3(AlSi_3O_{10})(OH,F)_2$	–	–	+	+	–
Talc, $Mg_3Si_4O_{10}(OH)_2$	–	–	–	–	–
Chlorite, $(Mg,Fe^{2+})_5Al(Si_3Al)O_{10}(OH)_8$	–	–	–	–	–
Kalifeldspar, $KAlSi_3O_8$	–	–	+	++	+
Plagioclase, $(Na,Ca)(Al,Si)_4O_8$	–	–	+	–	–
Leucite, $KAlSi_2O_6$				++	–
Quartz, SiO_2	–	–	+++	+++	+
Silicate glass	–	–	+++	+	–

Compared to the EAF-S, EAF-FD was enriched in CaO (36 wt%) and MgO (8.6 wt%). On the other hand, the TIC content accounted for 2.7 wt%, which corresponded to a $CaCO_3$ content of 23 wt%. Consequently, the CO_2 binding capacity accounted for 28 wt%, which was in the same range as for the slag. Ca is present in calcite (23 wt%), portlandite, fluorite and powellite. Portlandite (Duchesne and Reardon, 1995) and powellite (Khodokovskij and Mishin, 1971) have high solubilities at low pH. Mg was present as periclase (MgO), which gets covered by a brucite ($Mg(OH)_2$) layer in contact with water (Wogelius et al., 1995), which then controls solubility, and as spinel phases, i.e., $(Fe,Mg)(Al,Cr)_2O_4$, which are characterized by a rather low solubility (Höllen et al., 2016).

The BC-BA was characterized by a CaO content of 27 wt% with melilite as main Ca-containing phase. A calculation of the CO_2 binding capacity (Eq. (2)) yielded 24%.

Processed MSWI–BA contained melt products, unburnt residues, metals and glass. A laboratory experiment at the Fraunhofer Institute for Building Physics using electrodynamic fragmentation clearly demonstrated the capacity of this method to unlock intergrowth of particles of different fractions. It was shown that CaO was present predominantly in the melt products and therein especially in the melilite group phases. In contrast to these crystalline phases the glassy matrix, which made up 30–40% of the melt products, was depleted with an average CaO content of 23 wt% compared to melilite (28–39 wt% CaO) according to electron microprobe measurements of individual phases. MgO played a minor role with a bulk concentration of 3.7 wt% which was predominantly bound to melilite group phases. Melilite group phases were also the host for other elements like Fe (4.5 wt%), Al (5 wt%) and probably several heavy metals which would be released simultaneously in case of congruent melilite dissolution.

The PSI-A is significantly richer in Ca (54 wt% CaO) than the other investigated industrial residues. Combining qualitative XRD with quantitative XRF data showed that Ca was mainly bound to Ca-Olivine (22 wt%), but also in significant amounts of lime (9 wt%), calcite (8 wt%), gehlenite, tricalcium aluminate, and portlandite, whereas quartz (2 wt%) was the only Ca-free phase.

A comparison of the chemical analyses with literature data (Rekersdrees et al., 2014; Drissen, 2004; Lechner et al., 2010; Pan et al., 2008; Obernberger et al., 1997) clearly revealed a general plausibility of our analytical results.

3.2. Dissolution experiments

Dissolution of slags and ashes yielded acid solutions (V = 600 mL) and remaining dissolution residues. However, other chemical components (e.g. Fe_2O_3, Cr_2O_3) were also present in the solids and limited the application opportunities. Crystalline quartz was the major phase whereas the amorphous content was significant, but not dominant.

Weighing the residues revealed that almost 90% of the EAF-S, 35% of the BC-BA and only insignificant amounts of MSWI-BA dissolved. However, the enormous loss of ignition of 35 wt% in the dissolution residue of MSWI-BA, suggested that this sample also took up some water, leading to a mass increase. A mass balance of the dissolution experiments is presented in Fig. 2. The significant deviations that in some cases can be noticed with respect to the initial contents of specific elements may be due to experimental uncertainties, such as incomplete digestion and analytical errors.

During dissolution experiments Si was enriched in the dissolution residue whereas Ca and Mg were preferentially dissolved. Al and Fe showed an intermediate behaviour. The dissolved Ca concentrations of about 10–30 g/L were not controlled by the total amount of Ca in the system, as in all cases significant amounts of Ca (3–12 wt%) remained in the solid residue. However, there was a linear correlation between the total content and the dissolved concentration, which suggested that the dissolved Ca concentration was controlled by the dissolution kinetics. However, the different dissolved Ca concentrations could also be due to different mineral phases with different solubility in the dissolution residues. According to this interpretation the dissolution reaction was not complete after 180 min. For the trace elements, Ti and Cr were rather enriched in the residue, Pb and Zn were rather dissolved and P and Cu mostly showed an intermediate behaviour.

However, significant differences occurred between individual experiments which were due to different mineralogy of individual input materials which is discussed below. X-ray diffraction patterns clearly reveal that dissolution of EAF-S was an incongruent process. The Ca content of the residue (expressed as CaO) accounted only for 7 wt% compared to 31 wt% in the untreated slag which indicated the dissolution of Ca-bearing phases. XRD analyses showed that this Ca release was mainly due to dissolution of melilite group phases.

Contrarily, the SiO_2 content of the solid increased from 9 wt% to 13 wt%. The formation of a bulb in the XRD pattern ranging from about 18 to 28 °2Θ suggested the neoformation of an amorphous phase by precipitation from the aqueous solution, which was not present in the input material according to microscopic investigations. The low leachability of Si was probably controlled by the dissolution equilibrium of this newly formed amorphous silica phase and not by the dissolution equilibrium of the primary silicate phases. Interestingly, also quartz formed, which could be explained by the high temperatures of 90 °C, as for ambient temperatures usually only amorphous silica forms (Iler, 1979) due to the Ostwald step rule (van Santen, 1984). Spinels and calcium chromite were enriched in the dissolution residues which reflected their low dissolution kinetics and/or low solubility which led to the low leachability of Cr, and probably also of V. Contrarily, lime, magnesiowustite, Ca silicates and brownmillerite dissolved significantly and were depleted in the dissolution residue. This corresponded to the observed relatively high leachability of Ca, Mg and Fe, but also of P which can substitute for Si in silicate structures. The results of XRD analyses were confirmed by electron microprobe analyses with respect to the presence of quartz and spinel phases, powellite was found as an additional phase, whereas calciochromite was not found (Fig. 3).

The aqueous solution produced from the dissolution of EAF-S was characterized by a Ca concentration of 17.6 g/L, which was desired for subsequent carbonation, but also by a Fe concentration of 26.7 g/L. An incorporation of Fe in the carbonate would create a problem for certain applications. Comparing the overall amount of Ca in solution of about 11 g Ca, which is calculated from the concentration of 17.6 g/L, with the overall amount in the solid of only 0.27 g showed that preferential leaching of Ca occurred.

Dissolution of EAF–FD led to a decrease in the CaO content of the solid from 36.41 wt% to 3.42 wt%. As for the EAF-S, SiO_2 was enriched in the dissolution residue (19.53 wt%) compared to the original dust (6.25 wt%). Fe_2O_3 and Cr_2O_3 were also enriched in the residue as their contents increased from 27.66 wt% to 34.29 wt% and from 11.91 wt% to 21.92 wt%, respectively. XRD patterns suggested that Cr was bound in chromite, and iron in spinel/chromite and hematite as in the original material. Powellite and fluorite were unaffected by the dissolution experiment. The XRD pattern of the dissolution residue did not show the bulb characteristic for amorphous silica, but suggested an enrichment of ferrosilite. This means, that in contrast to the EAF-S, silicates did not dissolve incongruently and the residue consisted of dissolution relicts instead of neoformations.

The aqueous solution produced from the EAF–FD had a Ca concentration (19.6 g/L) similar to that of the EAF-S, but was characterized by a much lower Fe concentration (i.e. 7.5 g/L compared

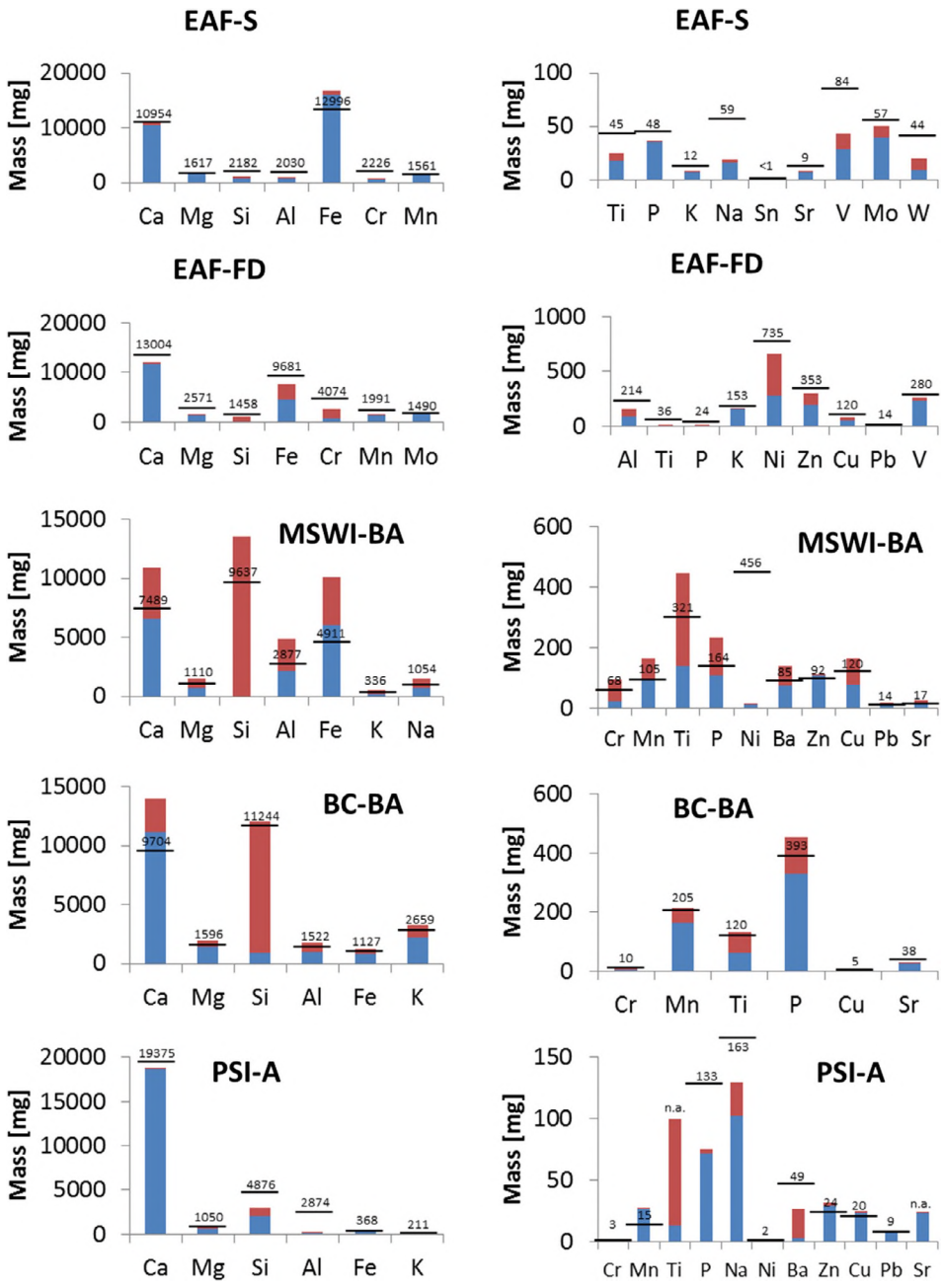

Fig. 2. Mass balance of dissolution experiments (left: main elements, right: trace elements; blue: dissolved amounts; red: amounts in dissolution residues; for sample abbreviations see Table 1; black lines: initial amounts in mg). (For interpretation of the references to colour in this figure legend, the reader is referred to the web version of this article.)

to 26.7 g/L). This difference might be due to the higher solubility of wustite compared to hematite, which was checked by hydrogeochemical modelling using Orchestra (Meeussen, 2003) and the Minteqv4 database (Felmy et al., 2004), but also due to a lower initial Fe content in the dust. Considering the high contents of Cr in the dissolution residue of the EAF-FD (22 wt%) (and to smaller degree also of the EAF-S, 5.6 wt%), a valorisation of this fraction as Cr concentrate in ferrous metallurgy seems possible.

As with the other input materials, the dissolution residue of biomass bottom ash was depleted in CaO with respect to the input material (from 27.17 to 11.99 wt%) and was enriched in SiO_2 (from 48.19 to 72.08 wt%). XRD patterns could explain this observation by the partial dissolution of melilite, $(Ca,Na)_2(Mg,Al)[Si_2O_7]$, leucite, $KAlSi_2O_6$, and apatite, $Ca_5[(F,Cl,OH)|(PO_4)_3]$, whereas quartz was enriched as a dissolution relict and silica mobilized from dissolution of the mentioned silicates re-precipitated as amorphous SiO_2.

Physical properties like compressive strength and abrasivity, which are relevant for a possible application as lightweight aggregate in concrete, could not be conducted due to too small sample amounts. However, the significant amorphous content might be connected with a certain hydraulic reactivity in building materials applications.

Dissolution of processed MSWI–BA yielded much higher solid to liquid ratios of Ca, Mg and Si compared to dissolution of the EAF-S, because less material was dissolved. XRD patterns suggested that melilite was preferentially dissolved whereas quartz was enriched in the dissolution residue.

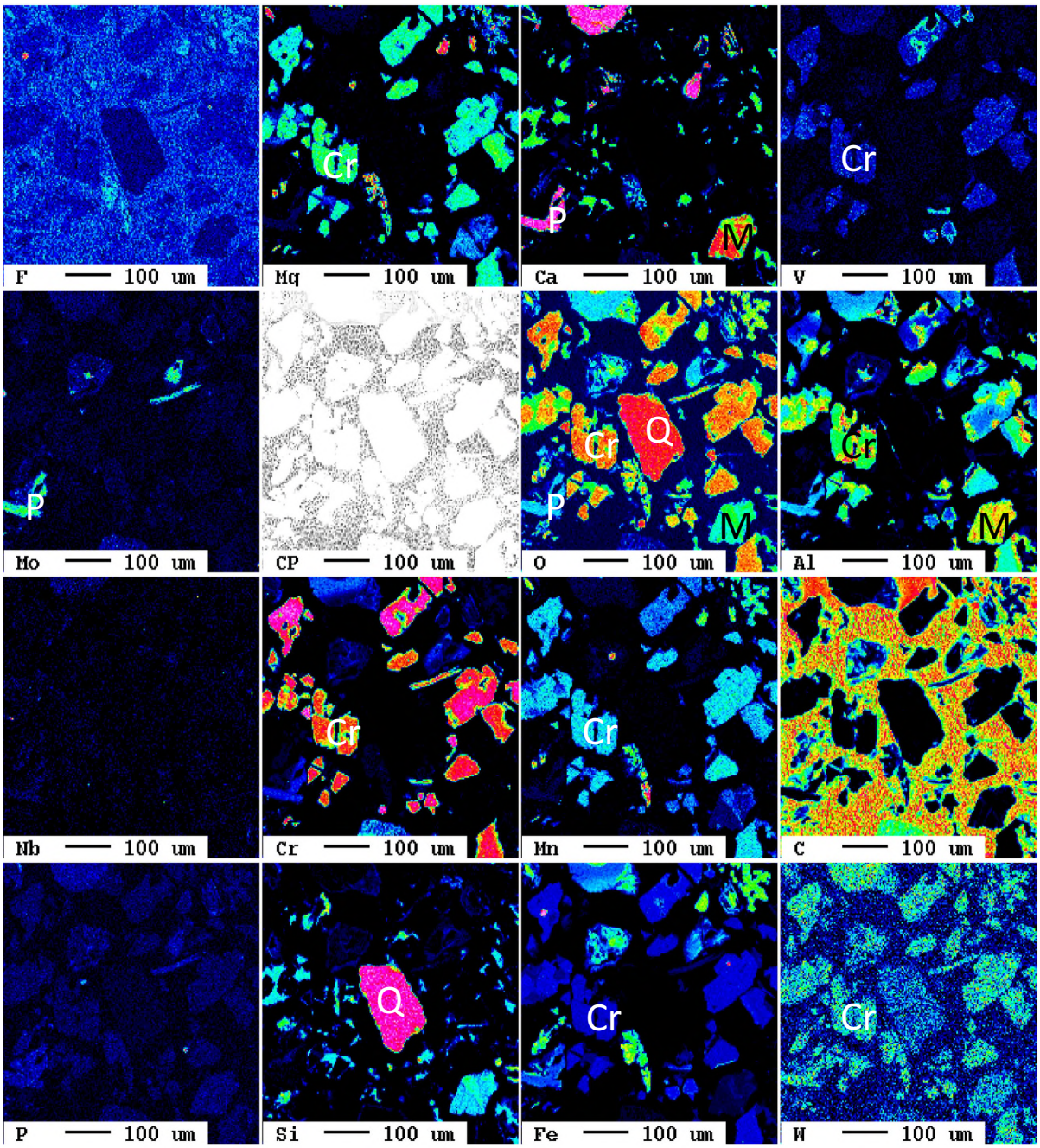

Fig. 3. Elemental distribution of F, Mg, Ca, V, Mo, O, Al, Nb, Cr, Mn, C, P, Si, Fe and W in the dissolution residue of an EAF-S showing the enrichment of spinels and quartz during the dissolution process (Q: quartz, Cr: chromium spinel, M: mayenite; P: powellite).

Dissolution of PSI-A led to an enrichment of SiO_2 in the residue. The decreased CaO/SiO_2 ratio in the residues suggested the dissolution of calcio-olivine which was present initially and the neoformation of amorphous silica.

Diffusion dialyses converted the strongly acidic experimental solution obtained from dissolution of serpentinte into an even more acidic hydrochloric acid which could be recycled and a partly neutralized solution containing the leached metals. The pH of the partly neutralized solution was +1.75 compared to −0.31 of the experimental solution and the conductivity decreased from 341 to 46 μS/cm. Diffusion dialyses was a good alternative to neutralisation by NH_3 addition, compared to which neutralisation time decreased from 5.5 h to 20 min and NH_3 consumption from 75 mL to 5 mL.

3.3. Precipitation experiments

Results of dissolution experiments clearly indicated high dissolved Fe concentrations (up to 27 g/L for EAF-S) in the resulting aqueous solutions which would have a negative effect on the quality of the subsequently produced carbonates. Titration with NH_3 almost completely removed Fe from the solution (by precipitating NH_4- and Fe-containing precipitates) (Fig. 4). This observation was in agreement with hydrogeochemical modelling using the database Minteqv4.dat and the modelling program Orchestra: At pH 9, the solubility of ferrihydrite, the iron phase which was most likely to precipitate due to the Ostwald step rule, was in the range of 1 nmol/L.

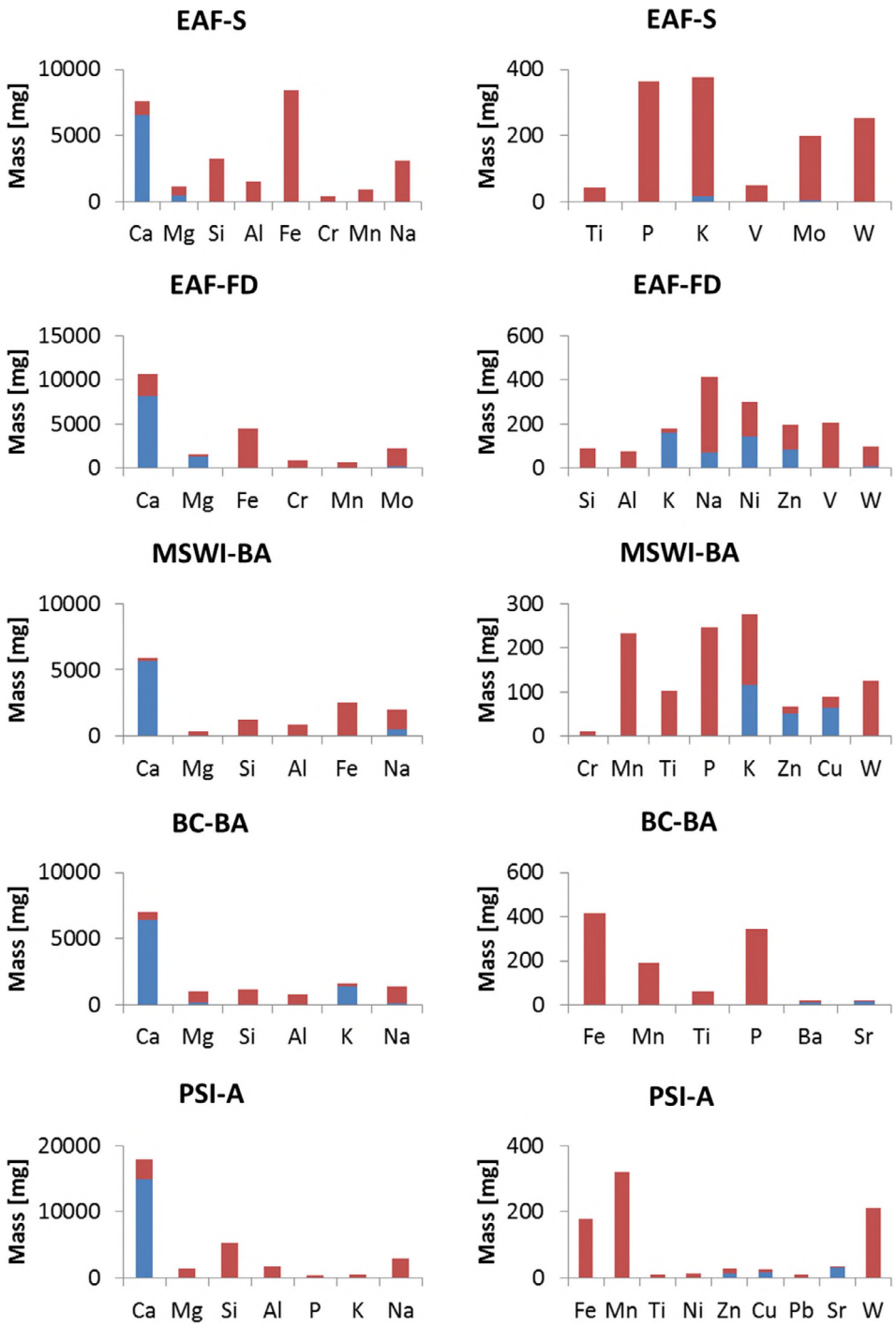

Fig. 4. Mass balance of precipitation experiments with NH_3 (left: main elements, right: trace elements; blue: dissolved amounts; red: amounts in precipitates; for sample abbreviations see Table 1). (For interpretation of the references to colour in this figure legend, the reader is referred to the web version of this article.)

Precipitation experiments clearly indicated for all input solutions that more than 80% of Ca remained in the solution, whereas Si, Fe and Al were precipitated. Among the trace elements, P, Mn, W and Ti were removed from the solution, whereas Cu, Zn and Sr remain in the solution. The precipitated elements were present in all the samples as highly soluble salt minerals. Additionally, in the experiments using EAF-S, EAF–FD and MSWI-BA iron hydroxides precipitated. Rinsing the precipitates with water would be required to use the precipitates in a blast furnace, as a first step to remove chlorides. Subsequently, sintering and possibly pelletizing could be applied to improve the mechanical properties for pig iron production. A direct use in electric arc steel making would not be possible as the metals occurred in their oxidized state and would need to be reduced in the blast furnace. In summary, technologically, a recycling of these fractions seems possible, but the effort for processing to enable their valorisation would be significant.

The addition of ammonia to the filtrate of the dissolution experiment of EAF-S triggered the precipitation of more than 40 g of a solid fraction. Interestingly, the only crystalline phase determined by XRD analyses was salammoniac, NH_4Cl, which means that all other chemical components were bound in amorphous phases or

below the detection limit. Assuming that chloride cannot form amorphous phases, a salammoniac percentage of 27 wt% and an amorphous fraction of 73 wt% were calculated. Elemental mapping using the electron microprobe confirmed the presence of a Fe-rich silicate gel as host phase for the other elements. Chemical analyses indicated that Fe was almost completely removed from the solution by adding ammonia.

Addition of ammonia to the solution derived from EAF-FD yielded a different type of precipitate compared to the experiment with EAF-S. According to the chemical analyses it was mainly composed of CaO, Fe_2O_3 and MoO_3, which are suggested to form phases like powellite or srebrodolskite. Thus, besides the desired removal of Fe, also a part of the dissolved Ca was removed undesirably.

As with the experiment using EAF-S, the experiment using MSWI–BA yielded salamonniac as the only crystalline precipitate, but its percentage was lower than in the precipitates of the EAF slag experiment. Chemical analyses suggested that the amorphous matrix should be an iron-rich silicate, but elemental mapping and EDX analyses showed very low Si concentrations and favoured the formation of a Fe—Al hydroxide. This contradiction might be explained by an inhomogeneous character of the precipitate where the selected samples for EMPA investigations were not representative.

Conditioning and beneficiation of the aqueous solution from BC-BA dissolution yielded not only salamonniac, but also ammonium carnallite, $NH_4MgCl_3{\cdot}6\ H_2O$ in similar quantities and sodium magnesium hydrogen phosphite as an accessory phase according to XRD measurements. However, SiO_2 and Al_2O_3 contents of approximately 15 and 8 wt% respectively, suggested the formation of an impure silica gel. According to elemental mapping using the electron microprobe, it was much poorer in Fe. The lower Fe content in the solid did not conflict with the almost quantitative removal of Fe from the solution due to the lower input concentration of Fe in the BC-BA.

Contrarily to the other input materials apart from EAF-FD, addition of ammonia to the aqueous solution derived from dissolution of PSI-A did not lead to the formation of salamonniac, but magnesium carnallite and sodium magnesium hydrogen phosphite formed. These phases also formed in the experiment with BC-BA, together with salamonniac. The other components, especially SiO_2, CaO, Al_2O_3, were incorporated in an x-ray amorphous gel-like phase. The iron content in the precipitate was lower compared to the other experiments, despite the almost quantitative removal from the solution.

3.4. Carbonation experiments

Injection of CO_2 in the filtrates which remained after separation of the metal concentrates resulted in precipitation of carbonates leaving behind Ca-depleted aqueous solutions with the exception of the experiment using PSI-A where significant Ca amounts remained dissolved (Fig. 5). Besides Ca also Al and Mn and Zn were fractionated into the precipitate, whereas K and Na remained in solution and Mg showed an intermediate behaviour. The main anion occurring in the solutions was chloride which was introduced during dissolution experiments and would require additional treatment. Remaining aqueous solutions also still contained environmentally relevant concentrations of heavy metals like Ni (up to 230 mg/L), Zn (up to 7 mg/L) or Cu (up to 65 mg/L), which would require further treatment prior to discharge. These treatments will require additional energy and costs which further decreases the economic and environmental performance of the entire process.

The solid products of carbonation were impure calcium carbonates with $CaCO_3$ contents ranging from 79 to 97 wt% (measured according to ÖNORM 13137), as indicated by ICP-MS analyses, XRD and electron microprobe analyses.

According to XRD analyses of the carbonate produced from EAF-S calcite, $CaCO_3$, was the only crystalline phase in the material and the amorphous content was negligible. Electron microprobe analyses suggested the incorporation of Mg in the calcite structure and only small traces of silicate phases were present, probably in quantities below the detection limit of XRD.

The produced carbonates were characterised by a $CaCO_3$ content of up to 97 wt% for the product from EAF-S which was very similar to the 98% purity reached for converter slagreached for converter slag in a previous study (Kodama et al., 2008). However, these slight differences would matter with respect to industrial applications as the minimum content for the paper industry is 98 wt% according to ÖNORM EN SO 3262-6.

Both the CaO and the TC content of the carbonate produced from EAF-FD were significantly lower than those of the carbonates produced from EAF-S. Unfortunately, the $CaCO_3$ content could not be determined directly, but was calculated from the TC content to be in the range of 59%. However, no other chemical components have been found by ICP-MS.

Chemical analyses of the carbonate produced from MSWI-BA indicated a $CaCO_3$ content of 79 wt%. However, XRD analyses showed calcium carbonates (mainly vaterite, some calcite) as the only crystalline phases. The XRD pattern did not show the characteristic bulb for amorphous silica, but both chemical analyses and electron microprobe analyses suggested such phases being present.

Carbonation of MSWI-BA occurs also naturally. On the one hand, this process is desired for application as building materials as it generally increases their chemical and physical stability (Fernández Bertoz et al., 2004). On the other hand, natural carbonation does not remove contaminants and the observed changes in mineralogy (Ohlsson, 2000) can also increase the leachability of certain elements. Furthermore, carbon storage is only restricted to the surface in natural carbonation processes. Contrarily, our experiments removed contaminants from the MSWI-BA, yielded a purer carbonate and stored a higher amount of CO_2.

The carbonate produced from BC-BA was very similar to that produced from MSWI-BA with respect to chemistry and purity, but calcite was the only $CaCO_3$ phase according to XRD analyses. The decrease in Cr concentration from 520 mg/kg in the initial BC-BA to 50 mg/kg in the carbonate showed exemplarily that for BC-BA, for which heavy metals may exceed the limit values (especially Cd, Cr and Zn (Obernberger et al., 1997; BMLFUW, 2001)), mineral carbonation might be a new recycling route to allow for agricultural use as liming agent.

The purity of the calcium carbonate produced from PSI-A was higher than that of the other ashes, but lower compared to EAF-S. The main crystalline phase was vaterite, whereas calcite only occurred in minor amounts. The impurities did not form crystalline phases according to XRD measurements which suggested a gel-like character. These results confirmed that the high CaO content of PSI-A (Sanna et al., 2014) makes them a feasible waste stream for the carbonation process which yielded higher purity products than other industrial residues.

Chemical analyses of the produced carbonates showed total carbon contents between 11 and 18 wt%. Considering the mass of the reaction products of about 9–14 g, their CO_2 content of about 40–67 wt% and the mass of the input materials of 50 g this meant that between 74 and 190 kg CO_2 per ton input material could be stored, which was significantly less than the calculated theoretical CO_2 uptake. The theoretical CO_2 uptake of a certain educt material was calculated from the CaO + MgO content, decreased by already present CO_2 in the educt material. The experimental CO_2 uptake was calculated from CO_2 contents and the weights of the reaction products (Table 3).

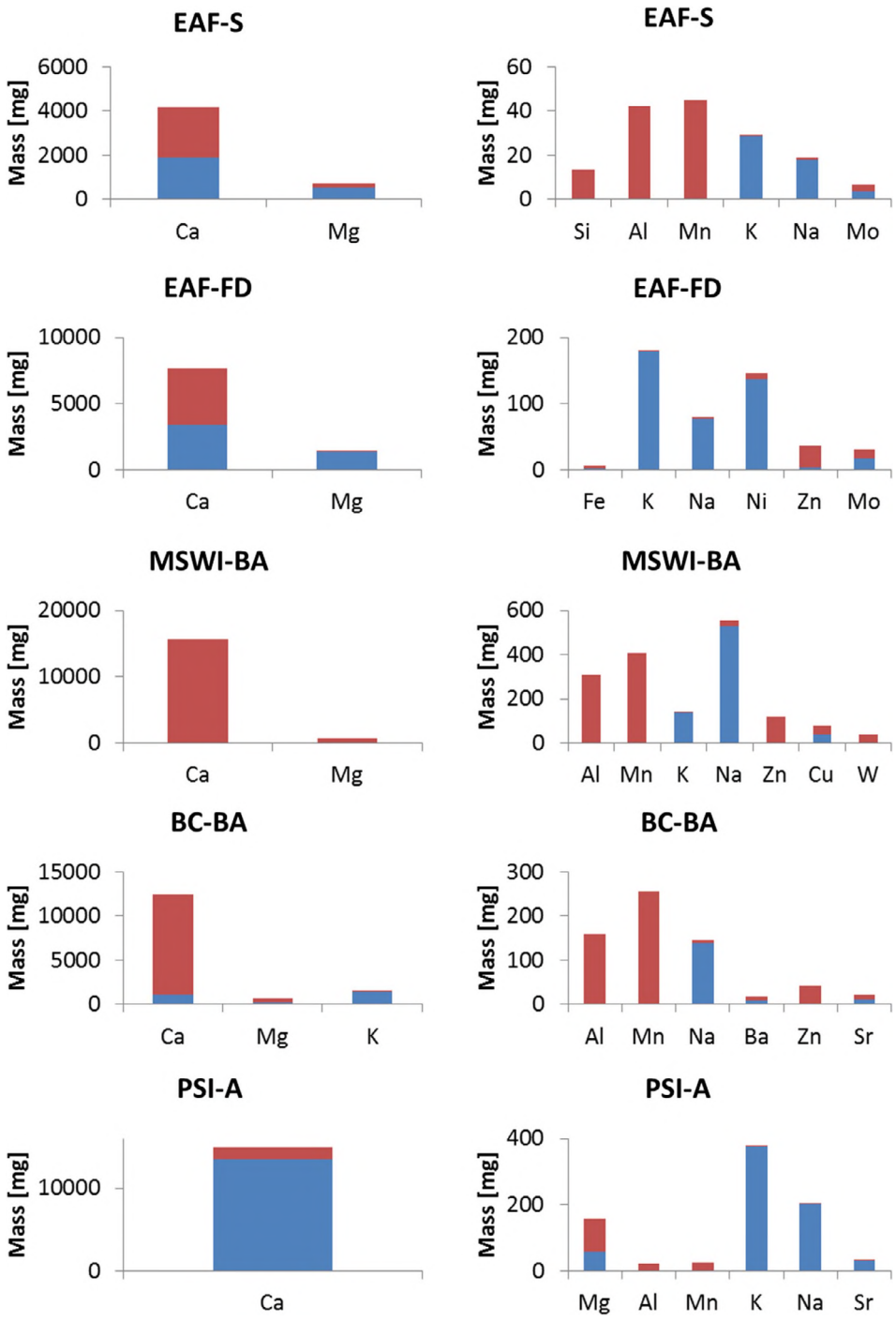

Fig. 5. Mass balance of carbonation experiments (left: main elements, right: trace elements; blue: dissolved amounts; red: amounts in precipitates; for sample abbreviations see Table 1). (For interpretation of the references to colour in this figure legend, the reader is referred to the web version of this article.)

Table 3
Experimental and theoretical CO_2 uptake of industrial residues for carbon capture and utilisation.

Parameter	EAF-S	EAF-FD	MSWI-BA	BC-BA	PSI-A[#]
Educt mass (g)	50	50	50	50	50
CaO (wt%)	30.67	36.41	20.97	27.17	54.25
MgO (wt%)	5.39	8.57	3.70	5.32	3.50
CO_2 (%)	<1.83	9.90	2.57	<3.67	n.a.
Theoretical CO_2 uptake (%)	28.26	28.15	18.02	23.57	n.a.
Product Mass (g)	14.3	9.3	9.8	8.6	10.4
CO_2 (%)	66.73	40.33	42.53	43.26	43.96
CO_2 (g)	9.54	3.75	4.17	3.72	n.a.
Experimental CO_2 uptake (% of input mass)	19.08	7.50	8.34	7.44	n.a.

The value of 19 g/100 g for EAF-S was in the same range as in experiments using ammonium salt solutions (16 g/100 g, 80 °C) (Kodama et al., 2008) or acetic acid followed by NaOH addition (23 g/100 g for blast furnace slag) (Eloneva et al., 2008a,b) and 9 g/100 g for LD slag (Eloneva et al., 2008a,b).

For MSWI-BA the achieved CO_2 binding capacity of 8 g/100 g was much higher than the 3 g/100 g observed in direct low liquid carbonation at a much coarser grain size of 4 mm 3 g/100 g (Rendek et al., 2006), but also higher than similar values observed for the direct liquid-solid route at 3 bar and a liquid/solid ratio between 0.3 and 0.4 (Fernández Bertoz et al., 2004). Slightly higher CO_2 binding capacities of 2–7 g/100 g were observed at 3 bar and a relative humidity of 75% for fly ashes, which are characterized by higher heavy metal contents (Li et al., 2007). Higher values of about 20 g/100 g have been reported for air pollution control residues (Cappai et al., 2012).

The CO_2 binding capacity observed for BC-BA was in the same range obtained in a direct carbonation experiment at 2 bar (8 g/100 g), whereas for the carbonation of PSI-A the range of 10–26 g/100 g (Gunning et al., 2010) was not reached.

Considering CO_2 capture, utilisation and storage (CCUS) the following estimate can be given: The production of 1 ton of ground limestone for agricultural purposes is related to the net emission of 59 kg C (West and McBride, 2005) which corresponds to 216 kg CO_2. The production of 1 ton of calcium carbonate via the suggested route is on the one hand associated with the uptake of about 74–191 kg CO_2. However, the CO_2 emissions during our process could not be specifically determined due to the enormous uncertainties (different grain size and hardness of input materials, differences between lab and real scale, effect of possible acid recyling, etc.). Therefore, it remains unknown, if these are above or below the total avoided emissions of 290-407 kg CO_2 per ton of limestone produced by this route in substitution of the traditional process. For this purpose, the desirable net comparison between CO_2 emissions of primary and secondary resources cannot be given for our approach. However, it is obvious that acid regeneration is required for a resource-efficient process. Our results suggest that diffusion dialysis is a feasible technology for this purpose, but would have to be compared with alternatives like electrochemical and membrane technologies.

Finally, it has to be stressed that the market requirements of the products were not yet met for high-value applications such as filler in the paper industry. This means that despite the availability of the initial residues, the feasibility of the overall process cannot be established at this stage. However, it seems more realistic that the treatment of these residues would be the driver for the entire process than the CO_2 storage which would be an extra benefit. For this purpose the leaching behaviour of the carbonation product and that of the silica rich by-product should be also examined besides their total content.

4. Conclusion and outlook

The aim of this work was to apply a stepwise mineral carbonation treatment to different types of poorly valorised industrial residues to assess which may be the most promising ones to employ for the process, in terms of total content of specific elements in the obtained products.

The selected approach yielded calcium carbonate with $CaCO_3$ contents between 79 and 97 wt%. For a detailed assessment of the utilisation options it is necessary to better characterize the carbonate product. EAF-S turned out to be a quite promising material for the suggested technology, as it yields on the one hand a ferrous metal concentrate and a very pure PCC. However, further research is needed to obtain purer products which allow for higher value applications. For this purpose, the process needs to be optimized for a specific residue and based on these results an assessment of the energy and material requirements, as well as environmental and economic assessment for the overall process, taking into account of the substitution of primary raw materials, could be performed. The main challenge will be to better remove Al_2O_3 during the precipitation stage and to develop a method for preventing Mg to co-precipitate from the solution. Considering material quality it also has to be mentioned that some heavy metal concentrations, like Zn (<0.08 wt%) are still too high in all the produced carbonates and that especially these metals fractionated into the carbonates during the stepwise process. Consequently, methods for their removal, for example precipitation as sulphides under reducing conditions, should be tested. Also the yield of carbonates needs to be enhanced, as in several elements significant residual Ca concentrations remained in solution.

Regarding the objectives of the project, the following main outcomes can be summarised:

1. The suggested stepwise treatment of ashes and slags which are currently disposed of in landfills, yielded first promising results with respect to the removal of contaminants like Cr from EAF-S or Pb from MSWI-BA. However, other contaminants like Zn could not yet be removed sufficiently.
2. Laboratory experiments demonstrated that between 74 and 191 kg CO_2 could be stored in 1 ton of industrial residue which shows a pathway to reduce the CO_2 emissions of Waste-to-Energy plants and other energy-intensive industrial plants by carbon capture, utilisation and storage (CCUS).
3. Precipitated calcium carbonate (PCC) with $CaCO_3$ contents of up to 97 wt% was produced, but further quality improvements are required to use it as a substitute for primary resources in the paper industry.
4. Dissolution experiments left behind a SiO_2 concentrate whose suitability for use as an aggregate for building materials could not be determined due to too small sample amounts.
5. A precipitate enriched in Fe and Cr was produced, but it contained also salts that may limit its applications as secondary raw materials for the metallurgical industry.

Acknowledgements

The authors thank Prof. Roland Pomberger and Prof. Peter Moser for their general support of the project, Robert Treimer for contributions to the project with respect to primary resources. We also want to thank our student assistant Katharina Pleßl for her help with literature research and dissolution/carbonation experiments, respectively, as well as the whole laboratory team of the Chair of Waste Processing Technology and Waste Management for chemical analyses. Many thanks to Dr. Federica Zaccarini, Sabine Feuchter, and Horst Hopfinger for mineralogical preparations and analyses. Special thanks is extended to Prof. Dr. Reto Gieré for the support during the stay of Philipp Sedlazeck at the University of Pennsylvania which was funded by the Marshall Plan Foundation to which we also express our thanks as well as the Austrian Research Promotion Agency which funded the project as "Research Studio Austria" CarboResources.

Role of the funding source

The Research Studio Austria *CarboResources* is funded by the Austrian Research Promotion Agency (FFG) (No. 844715). The FFG accepted the study design and the approach to collect, analyse and interpret the data by accepting the research proposal. However, the FFG was not involved in the realization of the project,

the writing of this article and the decision to submit this article for publication.

Appendix A. Supplementary material

Supplementary data associated with this article can be found, in the online version, at https://doi.org/10.1016/j.wasman.2018.06.048.

References

Adamcyzk, Burkart et al., 2010. Recovery of chromium from AOD-converter slags. Steel Res. Int. 81 (12), 1078–1083.

Austrian Federal Ministry of Agriculture, Forestry, Environment and Water Management. 2017. Federal Waste Management Plan, 2017.

BMLFUW, 2014a. Die Bestandsaufnahme der Abfallwirtschaft in Österreich. Statusbericht 2013. s.l. : Bundesministerium für Land- und Forstwirtschaft, Umwelt und Wasserwirtschaft, 2014. p. 95. http://www.bundesabfallwirtschaftsplan.at/dms/bawp/Statusbericht_2017/Statusbericht_2013.pdf.

BMLFUW, 2014b. Die Bestandsaufnahme der Abfallwirtschaft in Österreich. Statusbericht 2014. s.l.: Bundesministerium für Land- und Forstwirtschaft, Umwelt und Wasserwirtschaft, 2014, p. 94. http://www.bundesabfallwirtschaftsplan.at/dms/bawp/Statusbericht_2018/Statusbericht_2014.pdf.

BMLFUW, 2001. Verordnung über Qualitätsanforderungen an Komposte aus Abfällen (Kompostverordnung). Bundesministerium für Land- und Forstwirtschaft, Umwelt und Wasserwirtschaft. 2001. BGbl. II Nr. 292/2001.

BMLFUW, 2015. Die Bestandsaufnahme der Abfallwirtschaft in Österreich. Statusbericht 2015. Vienna: s.n., 2015.

Cabrera-Real, H. et al., 2012. Effect of MgO and CaO/SiO2 on the immobilization of chromium in synthetic slags. J. Mater. Cycles Waste Manage. 14, 317–324.

Cappai, G. et al., 2012. Application of accelerated carbonation on MSW combustion APC residues for metal immobilization and CO2 sequestration. J. Hazard. Mater. 207–208, 159–164.

Chairaksa-Fujimoto, R. et al., 2015. New pyrometallurgical process of EAF dust treatment with CaO addition. Int. J. Mineraly, Metall., Mater. 22 (8), 788–797.

Costa, G. et al., 2007. Current status and perspectives of accelerated carbonation processes on municipal solid waste combustion residues. Environ. Monit. Assess. 135, 55–75.

Drissen, P., 2004. Eisenhüttenschlacken – industrielle Gesteine. Report des FEhS – Institut für Baustoff-Forschung 1, 5.

Duchesne, J., Reardon, E.J., 1995. Measurement and prediction of portlandite solubility in alkaline solutions. Cem. Concr. Res. 25 (5), 1043–1053.

Eloneva, S. et al., 2008a. Fixation of CO2 by carbonating calcium derived from blast furnace slag. Energy 33, 1461–1467.

Eloneva, S. et al., 2012. Preliminary assessment of a method utilizing carbon dioxide and steelmaking slags to produce precipitated calcium carbonate. Appl. Energy 90, 329–334.

Eloneva, S. et al., 2008b. Steel converter slag as a raw material for precipitation of pure calcium carbonate. Ind. Eng. Chem. Res. 47 (18), 7104–7111.

Engström, F., Lidström Larsson, M., et al., 2014. Leaching Behaviour of Aged Steel Slags. Steel Res. Int. 85, 607–615.

Environmental Agency Austria, 2005. Abfallvermeidung und -verwertung: Aschen, Schlacken und Stäube in Österreich. Vienna: s.n., 2005. 3-85457-802-4.

Felmy, A., Girvin, D., Jenne, E., 2004. Minteq–a computer program for calculating aqueous geochemical equilibria. Environmental Protection Agency, Washington, D.C., 2004, Vols. EPA/600/3-84/032.

Fernández Bertoz, M. et al., 2004. Investigation of accelerated carbonation for the stabilisation of MSW incinerator ashes and the sequestration of CO2. Green Chem. 6 (8), 428–436.

Gara, S., Schrimpf, S., 1998. Behandlung von Reststoffen und Abfällen in der Eisen- und Stahlindustrie. Vienna: Umweltbundesamt, 1998, 3-85457-394-4.

Gunning, P.J., Hills, C.D., Cary, P.J., 2010. Accelerated carbon treatment of industria wastes. Waste Manage. (Oxford) 30, 1081–1090.

Höllen, D. et al., 2016. MiLeSlag - Zusammenhang von Mineralogie und Auslaugbarkeit von Stahlwerksschlacken. Schlacken-Symposium of Max Aicher Group. 2016, 125–139.

Huijgen, W.J.J., Witkamp, G.-J., Comans, R.N.J., 2005. Mineral CO2 sequestration by steel slag carbonation. Environ. Sci. Technol. 39, 9676–9682.

Iler, R.K., 1979. The Chemistry of Silica. Solubility, Polymerization, Colloid and Surface Properties, and Biochemistry. s.l.: Wiley, 1979.

Khodokovskij, I.L., Mishin, I.V., 1971. Solubility products of calcium molybdate and calcium tungstate; ratio of powellite to scheelite mineralization under hydrothermal conditions. Int. Geol. Rev. 13 (5), 760–768.

Kodama, S. et al., 2008. Development of a new pH-swing CO2 mineralization process with a recyclable reaction solution. Energy 33, 776–784.

Koukouzas, N.K. et al., 2006. Mineralogy and geochemistry of greek and chinese coal fly ash. Fuel 85, 2301–2309.

Lechner, P., Huber-Humer, M., 2011. Abfallwirtschaft und Abfallentsorgung - LV 813.100, Universität für Bodenkultur. Wien: s.n., 2011.

Lechner, P., Mostbauer, P., Böhm, K., 2010. Grundlagen für die Verwertung von MV-Rostasche - Teil A: Entwicklung des Österreichischen Behandlungsgrundsatzes. Institut für Abfallwirtschaft, Universität für Bodenkultur, 2010, p. 81. http://www.bmlfuw.gv.at/dms/lmat/greentec/abfall-ressourcen/behandlung-verwertung/behandlung-thermisch/Studien/BOKU_Grundsatz_Teil_A_Rostasche.pdf.

Li, X. et al., 2007. Accelerated carbonation of municipal solid waste incineration fly ashes. Waste Manage. (Oxford) 27, 1200–1206.

Ljung, A., Nordin, A., 1997. Theoretical feasability for ecological biomass ash recirculation: chemical equilbrium behaviour of nutrient elements and heavy metals during combustion. Environ. Sci. Technol. 31, 2499–2503.

Meeussen, J., 2003. ORCHESTRA: An object-oriented framework for implementing chemical equilibrium models. Environ. Sci. Technol. 37 (6), 1175–1182.

Meima, J.A. et al., 2002. Carbonation processes in municipal solid waste incinerator bottom ash and their effect on the leaching of copper and molybdenum. Appl. Geochem. 17 (12), 1503–1513.

Mulder, E., 1996. Pre-treatment of MSWI fly ash for useful application. Waste Manage. (Oxford) 16 (1–3), 181–184.

Muse, J.K., Mitchell, C.C., 1995. Paper mill boiler ash and lime by-products as soil liming materials. Agron. J. 87 (3), 432–438.

Nzihou, A., Sharrock, P., 2002. Calcium phosphate stabilization of fly ash with chloride extraction. Waste Manage. (Oxford) 22, 235–239.

Obernberger, I., Supancic, K., 2009. Possibilities of ash utilisation from biomass combustion plants. In: Proceedings of the 17th Biomass Conference & Exhibition, 2009.

Obernberger, I., et al., 1997. Beurteilung der Umweltverträglichkeit des Einsatzes von Einjahresganzpflanzen und Stroh zur Fernwärmeerzeugung. Institut für Verfahrenstechnik, Graz University of Technology. 1997. Jahresbericht 1995 z7um gleichnamigen Forschungsprojekt.

Ohlsson, K.E.A., 2000. Carbonation of wood ash recycled to a forest soil as measured by isotope ratio mass spectroscopy. Soil Sci. Soc. Am. J. 64 (6), 2155–2161.

Pan, J.R. et al., 2008. Recycling MSWI bottom and fly ash as raw materials for portland cement. Waste Manage. (Oxford) 28 (2008), 1113–1118.

Piantone, P., Bodénan, F., Chatelet-Snidaro, L., 2004. MIneralogical study of secondary mineral phases from weathered MSWI bottom ash: implications for the modelling and trapping of heavy metals. Appl. Geochem. 19, 1891–1904.

Pleßl, K., 2015. Holzaschen in Österreich. s.l.: Montanuniversität Leoben, 2015. Unpublished report.

Rekersdrees, T., Schliephake, H., Schulbert, K., 2014. Aufbau und Prozessführung des Lichtbogenofens unter besonderer Berücksichtigung des Schlackenmanagements. [book auth.] K.J. Thomé-Kozmiensky. Mineralische Nebenprodukte und Abfälle - Aschen, Schlacken, Stäube und Baurestmassen. Neuruppin : TK-Verlag 2014, 305–326.

Rendek, E., Ducom, G., Germain, P., 2006. Carbon dioxide sequestration in municipal solid waste incinerator (MSWI) bottom ash. J. Hazard. Mater. B128, 73–79.

Republik Österreich, 2015. Recycling-Baustoffverordnung. Bundesgesetzblatt, 2015.

Sanna, A. et al., 2014. A review of mineral carbonation technologies to sequester CO2. Chem. Soc. Rev. 43, 8049–8080.

Sanna, A. et al., 2012. Waste materials for carbon apture and storage by mineralisation (CCSM) - A UK perspective. Appl. Energy 99, 545–554.

Shi, C., 2004. Steel slag — its production, processing, characteristics, and cementitious properties. J. Mater. Civ. Eng. 16 (3), 230–236.

Suer, P. et al., 2009. Reproducing ten years of road ageing - Accelerated carbonation and leaching of EAF steel slag. Sci. Total Environ. 407, 5110–5118.

van Santen, R.A., 1984. The Ostwald step rule. J. Phys. Chem. 88, 5768–5769.

Vassilev, S.V. et al., 2013a. An overview of the composition and application of biomass ash. Part 1. Phase-mineral and chemical composition and classification. Fuel 105, 40–76.

Vassilev, S.V. et al., 2013b. An overview of the composition and application of biomass ash. Part 2. Potential utilisation, technological and ecological advantages and challenges. Fuel 105, 19–39.

West, T., McBride, A., 2005. The contribution of agricultural lime to carbon dioxide emissions in the United States: dissolution, transport, and net emissions. Agric. Ecosyst. Environ. 108, 145–154.

Wogelius, R. et al., 1995. Periclase surface hydroxylation during dissolution. Geochim. Cosmochim. Acta 59 (9), 1875–1881.